

Noise and Vibration: *Emerging Methods*  
**NOVEM 2009**  
5-8 April 2009 Oxford

## MODELLING THE VIBRATIONS OF CONVEX POLYGONAL PLATES BY THE IMAGE SOURCE METHOD

Jacques Cuenca\*, François Gautier, Laurent Simon

LAUM, CNRS, Université du Maine  
Avenue Olivier Messiaen, 72085 Le Mans 9, France  
Jacques.Cuenca.etu@univ-lemans.fr  
Francois.Gautier@univ-lemans.fr  
Laurent.Simon@univ-lemans.fr

### ABSTRACT

*The aim of this study is to investigate the capability of the image source method (ISM) for predicting medium and high frequency flexural vibrations of damped convex polygonal thin plates including various boundary conditions. Besides its classical use in room acoustics, ISM has already been applied to polygonal plates comprising simply supported and roller supported edges. Such boundaries include reflection coefficients that are independent from the angle of incidence of waves. In order to render ISM applicable to more complex boundary conditions, the existing formulation must be adapted. In this paper we present a new formulation of ISM which allows to include angle-dependent reflection coefficients. For practical implementation, an approximation consisting in neglecting edge effects is investigated. An example of implementation is presented and the interest of the method for high frequency vibration modelling is discussed.*

### 1 INTRODUCTION

Mainly, three different strategies are of common usage for modelling high-frequency structural dynamics. The first consists in extending existing low-frequency methods such as finite elements (FE) to higher frequency ranges, which is achieved either by improvement of computer hardware capabilities or by suitably post-processing or adapting FE models to high-frequencies (see Ref. [13] for example). The second strategy consists in modelling the averaged behaviour of the structure by energy methods such as statistical energy analysis (SEA) (see Refs. [10, 12]). These methods are well-suited for high frequency applications but are limited by the high number of preliminary hypotheses as input parameters. Hybrid FE-SEA methods also exist, for example consisting in separately describing long wavelength subsystems by FE and short wavelength subsystems by SEA (see Ref. [4]). The third strategy consists in computations by wave methods [16], i.e. involving the exact description of the vibrations as a sum of elementary waves. In this direction, one possible description of the flexural vibrations of plates is the image source method (ISM). The latter consists in the description of the vibrations of a polygonal domain excited by a point source as the superposition of the fields resulting from the original source and from its image sources relatively to the boundaries. For a given degree of accuracy to be reached, the number of needed image sources decreases with frequency [6], which renders the approach convenient for modelling systems in non-resonant regimes such as high frequency vibrations of plates.

The present study is based on a recent paper [2], which focuses on the capability of ISM to accurately compute the displacement field of polygonal plates in the case of simply supported boundaries. The method allows to analytically derive Green's functions of plates having particular polygonal geometries. It is also shown that the numerical implementation of ISM using a truncated series of image sources accurately predicts the high-frequency vibrating field of arbitrary convex polygonal plates with a limited number of image sources. The main limitation of the proposed method is that it exclusively applies to boundary conditions characterised by reflection coefficients that do not depend on the angle of incidence of waves, such as simply supported or roller supported boundaries. This is not the case for other kinds of boundary conditions such as clamped, free or elastically supported. In this paper we propose a formulation of ISM that allows to take into account boundary conditions that depend on the angle of incidence of waves.

## 2 STATEMENT OF THE PROBLEM

The system under study is a polygonal plate  $\Omega$  under the assumption of Kirchhoff's model for thin plates, represented in Fig. 1. The boundaries are denoted  $\partial\Omega$  and the plate is excited by a harmonic point source of unitary force at  $\mathbf{r}_0$ , normal to the plate surface. The space variable is denoted  $\mathbf{r}$ . The plate parameters are: Young's modulus  $E$ , Poisson coefficient  $\nu$ , density  $\rho$  and thickness  $h$ , which yield the bending stiffness of the plate

$$D = \frac{Eh^3}{12(1-\nu^2)} \quad (1)$$

and the wavenumber of flexural waves

$$k_f = \left( \omega^2 \frac{\rho h}{D} \right)^{1/4}, \quad (2)$$

where  $\omega$  is the circular frequency of the source. In the following, the  $e^{-j\omega t}$  time dependence is implicit. The displacement field  $w_\Omega$  of the plate is a solution of the set of equations

$$\begin{cases} D(\nabla^4 - k_f^4)w_\Omega(\mathbf{r}, \mathbf{r}_0; k_f) = \delta(\mathbf{r} - \mathbf{r}_0), & \mathbf{r} \in \Omega, \\ \text{Boundary conditions,} & \mathbf{r} \in \partial\Omega. \end{cases} \quad (3)$$

$$\quad (4)$$

The aim of the following is to determine  $w_\Omega$  by applying the image source method to the point source in the convex polygonal plate  $\Omega$ .

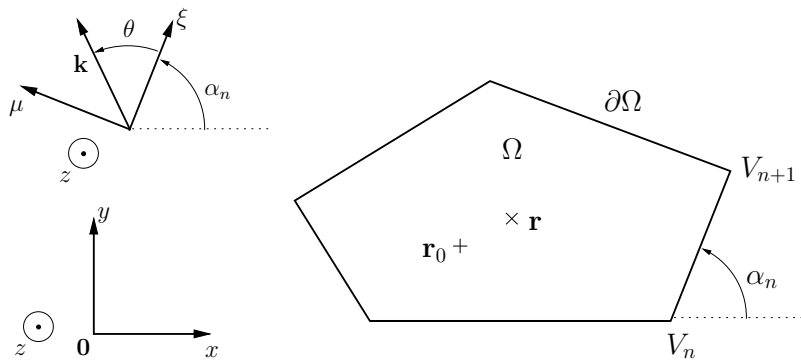


Figure 1: Global coordinate system  $(x, y)$  and local coordinate system  $(\xi, \mu)$  for edge  $n$  of polygonal plate  $(\Omega, \partial\Omega)$ .  $(V_n, V_{n+1})$ , vertices defining  $\xi$  axis;  $\mathbf{k}$ , wavenumber vector associated to a reflected plane wave on edge  $n$ .

### 3 ISM USING DIRECT APPROACH

The reflection coefficients associated to the different boundaries of the plate generally depend on the angle of incidence of waves. However, in some particular cases, such reflection coefficient is constant. For example, the reflection coefficients of simply supported and roller supported edges are respectively  $R = -1$  and  $R = 1$ . In such cases, the set of Eqs. (3) and (4) can be written [2]

$$D (\nabla^4 - k_f^4) w_\Omega(\mathbf{r}, \mathbf{r}_0) = \mathcal{D}_\Omega(\mathbf{r}, \mathbf{r}_0), \quad (5)$$

where  $\mathcal{D}_\Omega(\mathbf{r}, \mathbf{r}_0)$  contains an infinity of sources needed for satisfying the boundary conditions on  $\partial\Omega$ . The image sources model the successive reflections of waves on the boundaries. They are located outside the polygonal plate and are obtained by successive symmetries of the original source with respect to the boundaries, in the form

$$\mathcal{D}_\Omega(\mathbf{r}, \mathbf{r}_0) = \sum_{s=1}^{\infty} R^{N_r(s)} \delta(\mathbf{r} - \mathbf{r}_s), \quad (6)$$

where  $\mathbf{r}_s$  is the location of a given image source  $s$  and  $N_r(s)$  is the number of reflections needed for building source  $s$ . The solution to Eq. (5) is then

$$w_\Omega(\mathbf{r}, \mathbf{r}_0) = \mathcal{D}_\Omega(\mathbf{r}, \mathbf{r}_0) * G_\infty(\mathbf{r}, \mathbf{0}), \quad (7)$$

where  $G_\infty$  is the infinite plate Green's function. Eq. (7) allows to compute the Green's function of the flexural vibrations of any convex polygonal plate with simply supported or roller supported edges, which is developed in detail in Ref. [2]. The main limitation of such approach is that Eq. (6) is not applicable to reflection coefficients depending on the angle of incidence of waves on the boundaries, such as clamped or free edges. In the following, a different formulation of image sources is developed in order to render ISM applicable to more complex boundary conditions.

### 4 ISM USING FOURIER TRANSFORM APPROACH

The solution of Eqs. (3) and (4) is obtained as the superposition of the contributions from the original (real) source and its successive image (virtual) sources with respect to the boundaries. In the following, the contributions of the original and image sources are developed. Fig. 2 illustrates the different steps of the construction of the image source solution.

#### 4.1 Original source contribution

The original source contribution is modelled as the Green's function  $G_\infty$  of the associated infinite plate, which is the solution of the equation

$$D (\nabla^4 - k_f^4) G_\infty(\mathbf{r}, \mathbf{r}_0; k_f) = \delta(\mathbf{r} - \mathbf{r}_0) \quad (8)$$

and is obtained as [8]

$$G_\infty(\mathbf{r}, \mathbf{r}_0; k_f) = \frac{j}{8k_f^2 D} \left( H_0^{(1)}(k_f |\mathbf{r} - \mathbf{r}_0|) - H_0^{(1)}(jk_f |\mathbf{r} - \mathbf{r}_0|) \right), \quad (9)$$

where  $H_0^{(1)}$  denotes the Hankel function of the first kind of order 0 and  $|\mathbf{r} - \mathbf{r}_0|$  is the source-to-receiver distance. The first and second terms in  $G_\infty$  respectively represent propagative and evanescent cylindrical waves outgoing from the point source at  $\mathbf{r}_0$ . The displacement field corresponding to the original source is represented in Fig. 2(a).

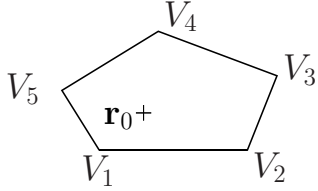
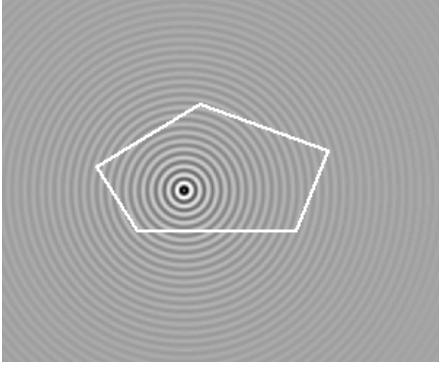
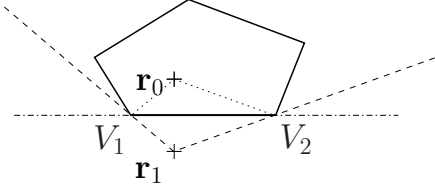
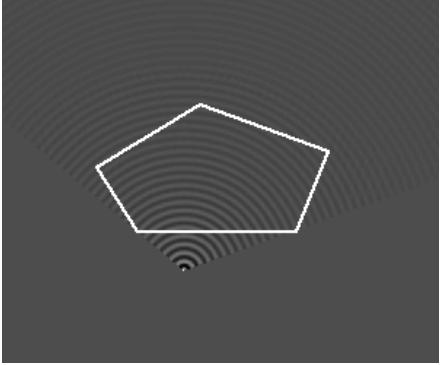
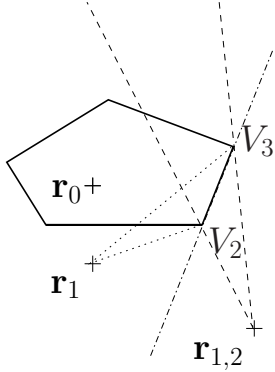

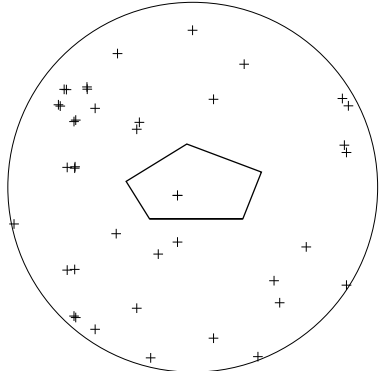
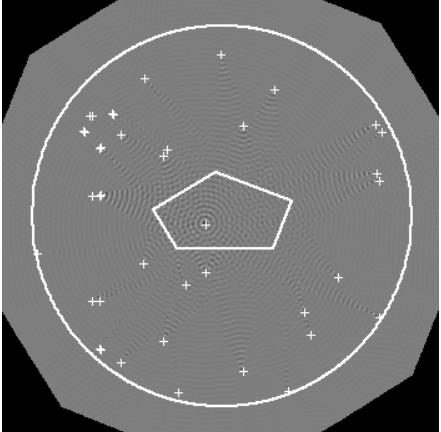
Computation step	Displacement field of sources
<p>(a)</p>  <p>Polygonal plate, original source and vertices</p>	 <p>Original source contribution; Eq. (9)</p>
<p>(b)</p>  <p>Construction of image source 1; Eqs. (15), (16)</p>	 <p>Image source 1 contribution; Eq. (21)</p>
<p>(c)</p>  <p>Construction of image source 1,2; Eqs. (15), (16)</p>	 <p>Image source 1,2 contribution; Eq. (21)</p>
<p>(d)</p>  <p>Truncation of the image source series; Eq. (23)</p>	 <p>Total field of the plate; Eq. (22)</p>

Figure 2. Image source model construction.

## 4.2 Image sources contributions

Image sources describe wave reflection on the plate boundaries. Each image source is defined by its location and its amplitude, which depend on the geometry and the boundary conditions of the plate. Most kinds of boundaries induce wave conversion from propagative to evanescent, and vice-versa. However, if the frequency of the excitation is sufficiently high, the effects of evanescent waves are relevant only in a small region near the boundaries. In the present method, image sources account for the propagative-to-propagative component of the reflected waves on the boundaries. Propagative-to-evanescent, evanescent-to-propagative and evanescent-to-evanescent reflections are ignored. The elements composing each image source are developed in the following.

### 4.2.1 Wave propagation

As in the case of the original source, wave propagation from image sources to the receiver is described by the Green's function of the associated infinite plate. The propagative-to-propagative component of the reflected field corresponding to image source  $s$  is given by the first term of the infinite plate Green's function  $G_\infty$  of Eq. (9),

$$g_s(\mathbf{r}, \mathbf{r}_s; k_f) = \frac{j}{8k_f^2 D} H_0^{(1)}(k_f |\mathbf{r} - \mathbf{r}_s|), \quad (10)$$

where  $\mathbf{r}_s$  is the location of source  $s$  (see section 4.2.3). The function  $g_s$  is the basic element for describing an image source. The weights of image sources, which depend on boundary conditions, are defined hereafter.

### 4.2.2 Amplitude of image sources

Each image source can be defined as a continuous sum of plane waves. Furthermore, the reflection of a plane wave on a plate boundary is characterised by a reflection coefficient which may depend on the angle of incidence of the plane wave [5]. The wavenumber vector associated to a reflected plane wave on edge  $n$  is denoted  $\mathbf{k}$ . The angle between edge  $n$  and  $\mathbf{k}$  is denoted  $\theta$ , as shown in Fig. 1. In order to separately describe wave reflection on each edge, a global coordinate system as a reference and a local coordinate system on each boundary are used. The global coordinates are denoted  $\mathbf{r} = (x, y)$ . The local coordinate system  $\mathbf{r} = (\xi, \mu)$  is such that  $\xi$  is collinear to the edge and  $\mu$  is oriented towards the inside of the plate (Fig. 1). In the same way, the wavenumber vector has the coordinates  $\mathbf{k} = (k_x, k_y)$  and  $\mathbf{k} = (k_\xi, k_\mu)$ . As a convention, the vertices  $V_n$  are numbered counterclockwise along the plate boundaries  $\partial\Omega$  and edge  $n$  corresponds to the segment between vertices  $V_n$  and  $V_{n+1}$ . Considering the propagation equation of a plane wave in an infinite plate, the dispersion relation of flexural waves in the plate is obtained as

$$k_f^4 = |\mathbf{k}|^4 = (k_x^2 + k_y^2)^2 = (k_\xi^2 + k_\mu^2)^2, \quad (11)$$

which implies the wavenumber components

$$k_\xi = k_f \cos(\theta), \quad k_\mu = k_f \sin(\theta). \quad (12)$$

The reflection coefficient of edge  $n$  for propagative waves is denoted  $R_n(\mathbf{k})$  in the local coordinate system  $\mathbf{k} = (k_\xi, k_\mu)$  and  $R_n(\mathbf{k}, \alpha_n)$  in the global coordinate system  $\mathbf{k} = (k_x, k_y)$ , where  $\alpha_n$  is the angle of orientation of edge  $n$ , as shown in Fig. 1. Such reflection coefficient can be represented as a function of the orientation  $\theta$  of an elementary plane wave and the frequency, such that  $R_n(\mathbf{k}) = R_n(\theta, \omega)$  in local coordinates. As an example, Fig. 3 shows the reflection coefficients of simply supported and clamped edges.

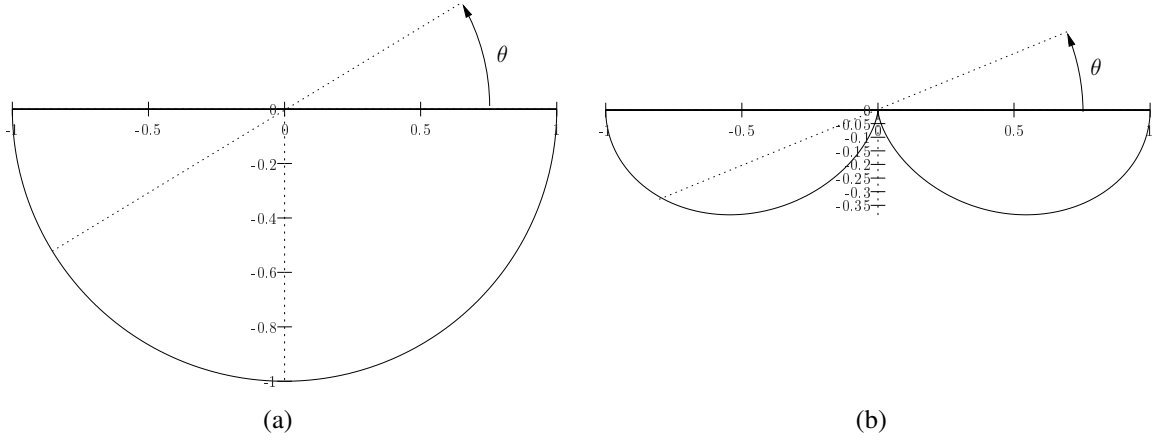


Figure 3: Real part of the propagative-to-propagative reflection coefficient  $R_n(\theta, \omega)$  in local coordinates of edge  $n$ . (a) Simply supported boundary; (b) clamped boundary.

A given image source  $s$  is obtained by successive symmetries of the initial source on the plate boundaries. The amplitude  $A_s$  of source  $s$  is therefore obtained as the product of the sequence of reflection coefficients  $R_n$ , in the form

$$A_s(\mathbf{k}) = \prod_{i=1}^{N_r^{(s)}} R_{n(i)}(\mathbf{k}, \alpha_{n(i)}), \quad (13)$$

where  $N_r^{(s)}$  number of reflections giving rise to source  $s$  and where  $n(i)$  is a sequence giving the order in which reflections take place. Using Eqs. (11) and (12),  $A_s$  can be written as

$$A_s(\mathbf{k}) = A_s(k_\xi, k_f) = A_s(\theta, \omega). \quad (14)$$

#### 4.2.3 Location of image sources

The location  $\mathbf{r}_s$  of image source  $s$  is obtained by successive symmetries of the initial source (located at  $\mathbf{r}_0$ ) on the plate edges. The source immediately giving rise to a new image source  $s$  is called the mother source  $m$  of  $s$ . Thus, for an image source  $s$  descending from  $m$ , it is convenient to note  $s = m, n$ , where  $n$  denotes the edge at which reflection occurs, also called the generator edge. The location  $\mathbf{r}_{m,n}$  of an image source is obtained from its mother source's location  $\mathbf{r}_m$  by the geometrical relation

$$\mathbf{r}_{m,n} = -\mathbf{r}_m + 2\mathbf{v}_n + 2 \frac{(\mathbf{r}_m - \mathbf{v}_n) \cdot (\mathbf{v}_{n+1} - \mathbf{v}_n)}{|\mathbf{v}_{n+1} - \mathbf{v}_n|^2} (\mathbf{v}_{n+1} - \mathbf{v}_n), \quad (15)$$

where  $\mathbf{v}_n$  and  $\mathbf{v}_{n+1}$  are the vertices of the generator edge. Furthermore, an image source  $s$  exists if it satisfies the boundary conditions at edge  $n$  with its immediate mother source  $m$  and if it is visible from an observation point  $\mathbf{r}$ . Such conditions of existence of image source  $s$  are included in the formulation by using the visibility window function

$$V(\mathbf{r}, \mathbf{r}_s) = \begin{cases} 1 & \text{in the visibility zone,} \\ 0 & \text{elsewhere.} \end{cases} \quad (16)$$

The geometrical construction of image sources is represented in Figs. 2(b) and 2(c).

### 4.3 Displacement field of the plate

#### 4.3.1 General expression

The displacement field of the plate is obtained by assembling the elements describing wave propagation and reflection and image source location. For a given image source  $s$ , its contribution to the displacement field of the plate is determined by the propagation function  $g_s(\mathbf{r}, \mathbf{r}_s; k_f)$ , the amplitude  $A_s(\mathbf{k})$ , the location  $\mathbf{r}_s$  and the visibility window  $V(\mathbf{r}, \mathbf{r}_s)$ .

The one-dimensional Fourier transform of a function  $w(\mathbf{r})$  in the local coordinate system  $\mathbf{r} = (\xi, \mu)$  of the generator edge of source  $s$  is defined as

$$\begin{cases} \bar{w}(k_\xi, \mu) = \mathcal{F}[w(\xi, \mu)]_{(k_\xi, \mu)} = \frac{1}{\sqrt{2\pi}} \int_{-\infty}^{+\infty} w(\xi, \mu) e^{-jk_\xi \xi} d\xi, & (17) \\ w(\xi, \mu) = \mathcal{F}^{-1}[\bar{w}(k_\xi, \mu)]_{(\xi, \mu)} = \frac{1}{\sqrt{2\pi}} \int_{-\infty}^{+\infty} \bar{w}(k_\xi, \mu) e^{jk_\xi \xi} dk_\xi, & (18) \end{cases}$$

It can be shown [5] that the Fourier transform of Eq. (10) is

$$\bar{g}_s(k_\xi, \mu; k_f) = \frac{j}{4\sqrt{2\pi}k_f^2 D} \frac{e^{-jk_\xi \xi_s} e^{j\sqrt{k_f^2 - k_\xi^2}|\mu|}}{\sqrt{k_f^2 - k_\xi^2}}, \quad (19)$$

which represents an elementary propagative plane wave. Thus, the plane wave that arises from source  $s$  is given by weighting  $\bar{g}_s(k_\xi, \mu; k_f)$  by the source's amplitude,  $A_s(k_\xi, k_f)$ . The displacement field in the spatial domain is given by inverse Fourier transform. Then, by including the visibility requirements at the receiver, the image source contribution to the total displacement field of the plate is

$$w_s(\xi, \mu, \xi_s, \mu_s; k_f) = V(\xi, \mu, \xi_s, \mu_s) \frac{1}{\sqrt{2\pi}} \int_{-\infty}^{+\infty} e^{jk_\xi \xi} A_s(k_\xi, k_f) \bar{g}_s(k_\xi, \mu; k_f) dk_\xi, \quad (20)$$

where coordinates  $(\xi, \mu)$  are local to the generator edge of each source  $s$ . Replacing  $\bar{g}_s$  by its explicit expression, the image source contribution takes the form

$$w_s(\xi, \mu, \xi_s, \mu_s; k_f) = \frac{j}{8\pi k_f^2 D} V(\xi, \mu, \xi_s, \mu_s) \int_{-\infty}^{+\infty} e^{jk_\xi(\xi - \xi_s)} A_s(k_\xi, k_f) \frac{e^{j\sqrt{k_f^2 - k_\xi^2}|\mu - \mu_s|}}{\sqrt{k_f^2 - k_\xi^2}} dk_\xi. \quad (21)$$

The total displacement field of the plate is then obtained as the superposition of the individual contributions from the sources, in the form

$$w_\Omega(\mathbf{r}, \mathbf{r}_0; k_f) = G_\infty(\mathbf{r}, \mathbf{r}_0; k_f) + \sum_{s=1}^{\infty} w_s(\mathbf{r}, \mathbf{r}_s; k_f). \quad (22)$$

#### 4.3.2 Truncation of the image source series

The number of sources that is needed for obtaining the displacement field of the plate by Eq. 22 is infinite. Thus, for practical usage, the image source series must be truncated [2]. The truncation criterion is such that sources taken into account are inside a truncation circle of radius  $r_t$  which is centred on the mean vertex location. For controlling the truncation, we use the dimensionless parameter

$$\gamma = \frac{r_t}{r_c}, \quad (23)$$

where  $r_c$  is an arbitrary distance of reference, taken as the mean free path of the plate [2], as

$$r_c = \frac{\pi S}{p}, \quad (24)$$

where  $S$  and  $p$  are, respectively, the surface area and the perimeter of the plate. The truncation of the image source series is illustrated in Fig. 2(d) for an arbitrary polygonal plate.

## 5 APPLICATION TO A POLYGONAL PLATE

The application of ISM using the direct approach (section 3) has been validated by comparison to FE simulations [2, 3] in the case of simply supported plates of arbitrary shape. Fig. 4 shows the displacement field of a steel triangular plate of vertices  $(0, 0)$ ,  $(0.75, 0)$ ,  $(0.5625, 0.9)$  (distances in meters) with thickness  $h = 2$  mm and damping ratio  $\eta = 0.07$ , for a point source at  $(0.3, 0.15)$  and an observation point at  $(0.45; 0.225)$ . Computation by ISM using direct approach with 793 sources ( $\gamma = 22.44$ ,  $r_c = 0.39$  m), compared to a FE model having 40534 nodes, leads to discrepancies that are less than 5%, which validates the approach.

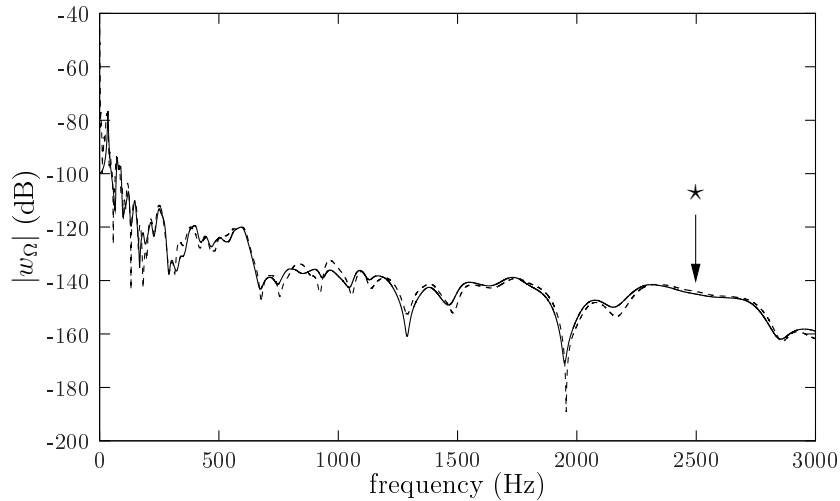


Figure 4: Displacement field of the plate. —, FE; - - -, ISM by direct approach; \*, frequency for computation of harmonic response of Fig. 5.

ISM using Fourier transform approach can be compared to ISM direct approach on the same triangular plate in order to validate the present method. Figs. 5(a) and 5(b) show the harmonic response of the triangular plate at 2.5 kHz computed by both approaches. The truncation parameter is chosen as  $\gamma = 2.5$ , which yields 34 sources. The displacement fields are found to be nearly identical. The difference can be quantified by using an error estimation, defined as

$$\text{error} = \left| \frac{w_{\Omega}^{(\text{Fourier})} - w_{\Omega}^{(\text{direct})}}{w_{\Omega}^{(\text{direct})}} \right|. \quad (25)$$

Such estimation is represented in Fig. 5(c). It can be observed that the error is near zero on almost the entire plate, except in regions such as the edges or the corners, where it reaches 5%. Such increase of the error is due to the fact that evanescent waves are not taken into account in the present method.

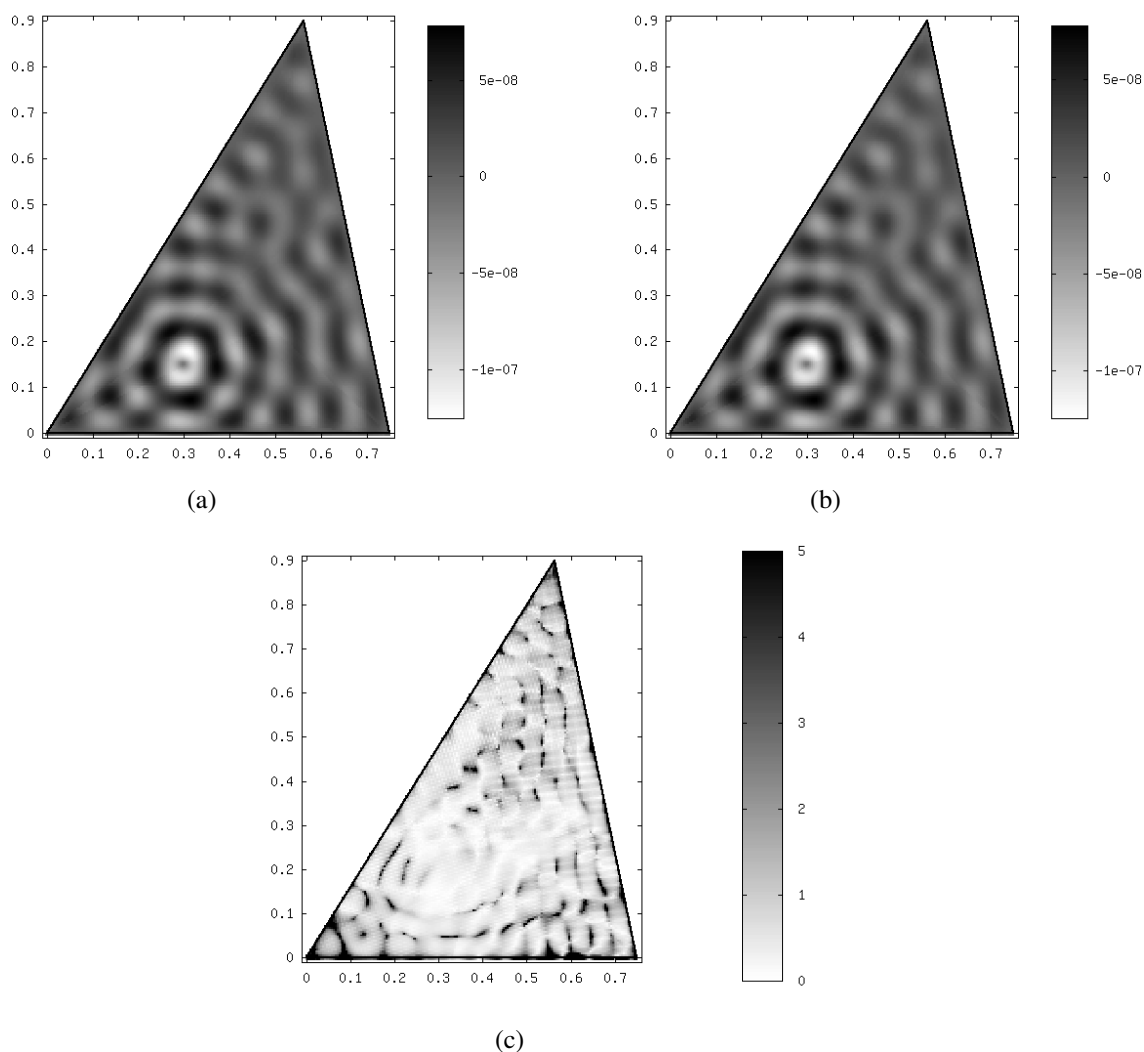


Figure 5: Harmonic response of the triangular plate at 2.5 kHz. (a) ISM using direct approach; (b) ISM using Fourier transform approach; (c) error, in percent.

## 6 CONCLUSION

In this paper, we have proposed a formulation of the image source method (ISM) for flexural vibrations of polygonal plates, which allows to include boundaries with angle-dependent reflection coefficients. The edge effects due to evanescent waves have been neglected in order to have a simplified approach. The advantage of the proposed method is that its accuracy increases with frequency and with structural damping. Such behaviour is opposite to those of classical FE methods. Therefore, ISM allows to reach high degrees of accuracy with a limited number of terms, i.e. image sources, which makes computations fast.

The most important result of this study is that ISM using Fourier transform approach gives equivalent results than ISM using direct approach. The latter is limited to simply supported or roller supported boundary conditions, which do not include a dependence on the angle of incidence of waves. The present approach allows to take into account such dependence. Work is in progress in order to take advantage of the applicability to the case of boundary conditions involving a dependence on the angle of incidence of waves.

## REFERENCES

- [1] J.R.F. Arruda, F. Gautier, L.V. Donadon, Computing reflection and transmission coefficients for plate reinforcement beams, *Journal of Sound and Vibration* 307 (2007) 564-577.
- [2] J. Cuenca, F. Gautier, L. Simon, The image source method for calculating the vibrations of simply supported convex polygonal plates, *Journal of Sound and Vibration* doi:10.1016/j.jsv.2008.11.018.
- [3] J. Cuenca, F. Gautier, L. Simon, Computing high frequency flexural vibrations of simply supported polygonal plates by the image source method, *Acoustics'08 Paris, second Acoustical Society of America and European Acoustics Association joint conference*, Paris, 29 June - 4 July 2008.
- [4] V. Cotoni, P. Shorter, R. Langley, Numerical and experimental validation of a hybrid finite element-statistical energy analysis method, *Journal of the Acoustical Society of America* 122(1) (2007) 259-270.
- [5] K.F. Graff, *Wave Motion in Elastic Solids*, Dover, New York, 1991.
- [6] R. Gunda, S.M. Vijayakar, R. Singh, Method of images for the harmonic response of beams and rectangular plates, *Journal of Sound and Vibration* 185(2) (1995) 791-808.
- [7] R. Gunda, S.M. Vijayakar, R. Singh, Flexural vibration of an infinite wedge, *Journal of the Acoustical Society of America* 102(1) (1997) 326-334.
- [8] R. Gunda, S.M. Vijayakar, R. Singh, J.E. Farstad, Harmonic Green's functions of a semi-infinite plate with clamped or free edges, *Journal of the Acoustical Society of America* 103(2) (1998) 888-899.
- [9] P. Ladevèze, The variational theory of complex rays for the calculation of medium-frequency vibrations, *Engineering with Computers* 18 (1999) 193-214.
- [10] A. Le Bot, A vibroacoustic model for high frequency analysis, *Journal of Sound and Vibration* 211(4) (1998) 537-554.
- [11] A.W. Leissa, *Vibration of Plates*, Acoustical Society of America, London, 1993.
- [12] R.H. Lyon, R.G. Dejong, *Theory and Application of Statistical Energy Analysis*, Butterworth-Heinemann, Boston, 1995.
- [13] B.R. Mace, D. Duhamel, M.J. Brennan, L. Hinke, Finite element prediction of wave motion in structural waveguides, *Journal of the Acoustical Society of America* 117(5) (2005) 2835-2843.
- [14] F.P. Mechel, Improved mirror source method in room acoustics, *Journal of Sound and Vibration* 256(6) (2002) 873-940.
- [15] W. Soedel, *Vibrations of Shells and Plates*, Marcel Dekker, New York, 1981.
- [16] C. Vanmaele, D. Vandepitte, W. Desmet, An efficient wave based prediction technique for plate bending vibrations, *Computer Methods in Applied Mechanics and Engineering* 196 (2007) 3178-3189.